THE JOURNAL OF PHYSICAL CHEMISTRY B

Article

pubs.acs.org/JPCB

Investigation of Methanol–Peptide Nuclear Overhauser Effects through Molecular Dynamics Simulations

J. T. Gerig*

Department of Chemistry & Biochemistry, University of California, Santa Barbara, Santa Barbara, California 93106, United States

Supporting Information

ABSTRACT: Intermolecular nuclear Overhauser effects (NOEs) produced by interactions of methanol with [val^5]angiotensin in 25% methanol–water at 0 °C were examined through molecular dynamics (MD) simulations and compared to experimental results. Calculated average $^3J_{NHC\alpha H}$ spin coupling constants, conformation-sensitive chemical shift changes, and intramolecular ^{1}H–^{1}H NOEs indicated that peptide conformations present over the course of simulation trajectories of 100–300 ns are likely similar to those present in the experimental system. Calculated cross-relaxation terms for the methanol–peptide interactions showed the same trends as corresponding experimental data but were about a factor of 3 too large. The lack of agreement between observed and calculated cross-relaxation terms probably has origins in characteristics of the simulations that lead to overestimation of translational diffusion coefficients of the system components. Simulations confirmed the heterogeneity of the methanol–water solvent at the molecular level, with clusters of methanol and water molecules changing their size and composition on a subpicosecond time scale. Most peptide hydrogens are preferentially solvated by interactions with methanol molecules. Simulations suggest that diffusion of water and methanol molecules near the peptide is slowed as these species approach the peptide backbone.

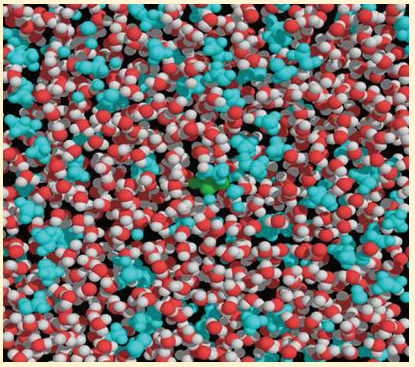

INTRODUCTION

Peptides and other biopolymers are dissolved in mixtures of water and small organic molecules for a variety of reasons. Often the organic component of the solvent is needed to enhance the solubility of another component of the system, perhaps a material that will react or interact with the biopolymer. The amount and identity of the organic component in a solvent may also be used to alter interactions with chromatographic media, influence the dominant conformation, alter motions critical to function, or encourage self-assembly.[1−3] Direct interactions between the organic component of a mixed solvent and a protein or peptide are presumably present to some extent but are usually ignored. It is possible to explore such interactions through intermolecular nuclear Overhauser effects (NOEs).[4−10]

A solvent proton–peptide proton NOE depends on an intermolecular cross-relaxation parameter (σ_{HH}^{NOE}). Interpretation of experimental cross-relaxation parameters can be based on the formulation of Ayant et al.[11] In their model, the solute proton of interest is considered to be located in a sphere of radius r_H, while the solvent spin is situated in a sphere of radius r_S. The intermolecular cross-relaxation rate is given by

$$\sigma_{HH}^{NOE} = \frac{3\gamma_H^4 h^2 N_S}{10\pi D r}(6J_2(2\omega_H) - J_2(0)) \quad (1)$$

where ω_H is the proton Larmor frequency; N_S is the number of solvent spins per milliliter; D is the sum of the translational diffusion coefficients for the molecules containing the peptide and solvent spins ($D = D_H + D_S$); r is their distance of closest approach ($r = r_H + r_S$), and $J_2(\omega)$ is a spectral density function (eq 2)

$$J_2(\omega) = (\omega\tau + \frac{5}{\sqrt{2}}(\omega\tau)^{1/2} + 4) \div [(\omega\tau)^3 + 4\sqrt{2}(\omega\tau)^{5/2} + 16(\omega\tau)^2 + 27\sqrt{2}(\omega\tau)^{3/2} + 81\omega\tau + 81\sqrt{2}(\omega\tau)^{1/2} + 81] \quad (2)$$

with the correlation time $\tau = r^2/D$. The magnetic dipole–magnetic dipole interaction is strongly dependent on the distance between interacting spins; it is the solvent spins closest to the solute proton that are largely responsible for relaxation.

Using eq 1 with experimental bulk translational diffusion coefficients and solvent component concentrations, in concert with reasonable conformations of a peptide solute, produces calculated cross-relaxation terms that are often in agreement with experimental observations. Disagreement between the predictions of eq 1 and experiment could signal that (1) local concentrations of the solvent components (N_S) are different from the bulk concentrations, (2) mutual diffusion of the solute and solvent is not well-described by the bulk diffusion coefficients (D_H, D_S), or (3) a conformation or conformation(s) of the

Received: November 17, 2011
Revised: January 17, 2012
Published: January 18, 2012

dx.doi.org/10.1021/jp211098v | J. Phys. Chem. B 2012, 116, 1965–1973

peptide solute, reflected in r_H and r_S, is/are different from the structures considered. Given how parameters related to these considerations enter eq 1, it may be difficult to develop a unique interpretation of a disagreement between an experimental σ_{HH}^{NOE} and one predicted from eq 1.

Molecular dynamics (MD) simulations of NMR relaxation phenomena have generally led to predictions of NMR relaxation and cross-relaxation behavior that are in reasonable accord with experiment.[12,13] We report here the results of MD simulations intended to help elucidate variations in methanol proton−peptide proton cross-relaxation terms for the octapeptide hormone [val^5]angiotensin II dissolved in 25% methanol/water (v/v).

Angiotensin II plays a central role in the renin−angiotensin−aldosterone system of blood pressure regulation.[14] The hormone exerts a variety of physiological effects by interacting with a number of specific receptors.[15,16] Solvation−desolvation effects may have a significant role in such binding.[17] Development of pharmaceutical interventions in this system has focused on the structure and dynamics of the peptide in solution and when bound to its receptors.[18−20] Such efforts have included MD simulations.[21,22]

$$H_3N^+-Asp_1\text{-}Arg_2\text{-}Val_3\text{-}Tyr_4\text{-}Val_5\text{-}His_6\text{-}Pro_7\text{-}Phe_8-COO^-$$
[val^5]angiotensin II

EXPERIMENTAL SECTION

Experimental determination of cross-relaxation parameters σ_{HH}^{NOE} for interactions between methanol CH_3 protons and protons of [val^5]angiotensin dissolved in 25% methanol−water (v/v) at 273 K have been previously reported.[23] The water portion of the solvent was a mixture of 85% H_2O and 15% D_2O (v/v). The sample was approximately 10 mM in peptide and contained trace amounts of acetate and 3-(trimethylsilyl)-propionic acid-d_4; the apparent pH was 3.1.

MD Simulations. All simulations were done with the GROMACS package[24,25] running on a SUN SunFire X4600. The AMBER99SB-ILDN force field was used for [val^5]-angiotensin.[26,27] The peptide terminals and the Asp, Arg, and His side chains were ionized in the model.[28] The Cornell et al. model of methanol[29] and the TIP4Pew model of water[30] were used.

A cubic simulation cell, approximately 9.7 nm on a side, was used. It contained a solute molecule, 3812 methanol molecules, 23 546 water molecules, and a chloride ion to maintain electrical neutrality. The integration time step was 0.002 ps. The PME method for long-range electrostatics was applied, as was the long-range correction for the van der Waals interaction described by Allen and Tildesley.[31] Cut-offs for electrostatic and van der Waals terms were 1.3 nm. The nonbonded interaction list was updated every 10 steps. Periodic boundary conditions were applied. The motion of the model center of mass was corrected every 10 steps. Snapshots of system coordinates and velocities typically were written every 0.2 or every 10 ps. Covalent bonds were constrained to constant length by the LINCS procedure; it was observed that removing these constraints had virtually no effect on the calculated cross-relaxation parameters. Systems were regulated at 273 K and a pressure of 1 bar by use of the Berendsen temperature (velocity rescaling) and pressure coupling methods with relaxation time constants of 0.1 and 1 ps, respectively.[32] Simulations to produce trajectories of 2−300 ns duration were carried out after initial equilibration for at least 2 ns.

Simulations in which snapshot of trajectories were taken at 0.2 ps intervals were used to examine the initial decay of correlation functions and diffusion of solvent components near the peptide. To account for the heterogeneities of the methanol−water system, ten different configurations of the system, taken at regular intervals from a 100 ns duration simulation, were used as starting points for a series of 2 ns simulations. Results calculated from the 10 trajectories were averaged. For study of slower phenomena, trajectories of 100−300 ns duration were calculated, with snapshots taken every 10 ps.

Analyses of Trajectories. Programs contained within the GROMACS package were used to compute the system density and self-diffusion coefficients of the solvent components using the Einstein relationship.[33] GROMOS routines were also used for clustering studies and for the calculation of spin coupling constants and conformation-dependent proton chemical shift changes. Locally developed programs were used to determine average peptide interproton distances and to compute spin dipolar interactions.

Abragam has shown that the spin−lattice relaxation cross-relaxation rate σ_{AB} arising from the dipolar interaction of a pair of distinguishable spin 1/2 particles A and B is given by eq 3[34]

$$\sigma_{AB} = \frac{3}{4}\gamma_A^2\gamma_B^2\hbar^2\left\{-\frac{1}{12}j^0(\omega_A - \omega_B) + \frac{3}{4}j^2(\omega_A + \omega_B)\right\} \quad (3)$$

Here, μ_0 is the permittivity of free space; γ is the proton gyromagnetic ratio; and ω_A and ω_B are the corresponding Larmor frequencies. The spectral density functions $j^m(\omega)$ are Fourier transforms of correlation functions $g^m(t)$ which can be written in terms of the components of the vector $\mathbf{r}$ which connects the two spins[12]

$$j^m(\omega) = 2\int_0^\infty g^m(t)e^{-i\omega t}dt = 2\int_0^\infty \langle F^m(0)F^{m*}(t)\rangle e^{-i\omega t}dt \quad (4)$$

with

$$F^0 = \frac{r^2 - 3z^2}{r^5} \quad F^1 = \frac{z(x - iy)}{r^5} \quad F^2 = \frac{(x - iy)^2}{r^5}$$

Random isotropic motion of the orientation of the vector $\mathbf{r}$ is assumed, with brackets indicating that the average of the quantity $F^m(0)F^{m*}(t)$.

Assuming that cross correlation effects are negligible,[35,36] the collective relaxation contributions to σ_{AB} by a group of identical B spins is given by

$$\sigma_{AB} = \frac{3}{4}\gamma_A^2\gamma_B^2\hbar^2\left\{-\frac{1}{12}J^0(\omega_A - \omega_B) + \frac{3}{4}J^2(\omega_A + \omega_B)\right\} \quad (5)$$

dx.doi.org/10.1021/jp211098v | J. Phys. Chem. B 2012, 116, 1965−1973

with

$$J^m(\omega) = 2\int_0^\infty G^m(t)e^{-i\omega t}dt = 2\int_0^\infty \langle\{\sum_{j\neq i}^{N_{cut}} F_{ij}^m(0)F_{ij}^m(t)\}\rangle e^{-i\omega t}dt \quad (6)$$

The summation in eq 6 collects all pairwise interactions with the target A spin which are then averaged over the sample.

The strong internuclear distance dependence of $G^m(t)$ dictates that σ_{AB} is dominated by interactions of a given target spin with its near-neighbor B spins. To reduce the computational effort required to evaluate $J^m(\omega)$, it is advantageous to limit the number of B spins considered to those spins that lie within a cutoff distance (r_{cut}) from the A spin. There will be N_{cut} B spins within this sphere. For the present work, we considered all interactions of a particular solute spin with methanol CH_3 protons that were within 3 nm of the solute spin.

For isotropic liquids, normalized correlation functions ($G^m(t)/G^m(0)$) are independent of m and have the same time dependence.[34] Following Feller et al.,[37] we assumed that the normalized functions can be represented by a collection of n exponentially decaying functions

$$\frac{G^m(t)}{G^m(0)} \cong \sum_n a_n \exp\left(-\frac{t}{\tau_n}\right) \quad (7)$$

By approximating the decay of $G^m(t)/G^m(0)$ in this way, the Fourier transform of $G^m(t)$ becomes

$$J^m(\omega) = 2G^m(0)\tau_m(\omega) \quad (8)$$

with

$$\tau_m(\omega) = \sum_n \frac{a_n\tau_n}{(1 + (\omega\tau_n)^2)} \quad (9)$$

where $\Sigma_n a_n = 1$.

Collecting terms, the cross-relaxation rate (σ_{HH}^{NOE}) arising from methanol−peptide protons in the present work is given by

$$\sigma_{HH}^{NOE} = -7.120\times10^{-8}G^0(0)\tau_0(0) + 6.408\times10^{-7}G^2(0)\tau_2(2\omega) \quad (10)$$

The units for $\tau_0(0)$ and $\tau_2(2\omega)$ are picoseconds.

Fitting of $G^m(t)/G^m(0)$ computed from a MD trajectory to a sum of exponential functions used a local version of Provencher's program DISCRETE.[38] (See http://s-provencher.com/index.shtml.) The program tried sums of up to eight terms, with the best fit selected according to criteria discussed by Provencher. Typically, the optimum fit to the decay of $G^m(t)/G^m(0)$ used 3 to 5 exponential terms, with the estimated errors of the fitting parameters typically ranging from 2% to 6%.

To compute $G^m(t)$ for a specific proton of the peptide, methanol CH_3 protons within 3 nm of the proton of interest in the simulation box were determined in a trajectory snapshot taken at a time defined as $t = 0$. Diffusion of the selected solvent protons was followed in subsequent snapshots with the quantities F^0, F^1, and F^2 evaluated at each time step (t). The quantity $F_{ij}{}^m(0)F_{ij}^m(t)$ was evaluated and stored so that it was associated with the time t. The snapshot chosen to represent $t = 0$ was then advanced one frame along the trajectory and the process repeated. Resulting $F_{ij}^m(0)F_{ij}^m(t)$ values at a given time were averaged. For a simulation producing a trajectory of 0.3 μs length and sampled at 10 ps intervals, the correlation function was represented by 700 to 1000 points obtained in calculations that averaged about 29 000 evaluations of each point. The number of methanol methyl protons (N_{cut}) within the 3 nm radius selection sphere ranged from 989 to 1939 but averaged 1382 ± 16 (461 ± 5 methanol molecules). A homogeneous 25% methanol−water solvent mixture at 0 °C contains 1390 methanol methyl hydrogens within a 3 nm sphere.

RESULTS

Density and Translational Diffusion. System density and translational diffusion coefficients of system components computed from simulations of 25% methanol−water are compared to experimental values in Table 1. The density is predicted well by the simulations, but translational diffusion coefficients are about 50% too large. The solute diffusion coefficient has a high uncertainty because the behavior of only a single molecule is calculated for each simulation run, while the behaviors of thousands of solvent molecules are averaged for each run to produce solvent diffusion data. The presence of peptide has no significant influence on the bulk diffusion of either water or methanol in the solvent mixture.

Table 1. Properties of 25% Methanol−Water (v/v) at 0 °C

property	no solute[a]	[Val^5]angiotensin[b]	experimental
density, g L^{-1}	975.9 ± 0.2	976.7 ± 0.1	971.9[c]
$D_{H2O} \times 10^{10}$, m^2 s^{-1}	8.68 ± 0.09	8.63 ± 0.14	5.90[d], 6.7[e]
$D_{MeOH} \times 10^{10}$, m^2 s^{-1}	7.43 ± 0.08	7.56 ± 0.18	4.97[d], 5.0[e]
$D_{Peptide} \times 10^{10}$, m^2 s^{-1}	-	1.0 ± 0.2	0.67[d]

[a]Simulation system contained only methanol and water. [b]Simulation system included one molecule of [val^5]angiotensin II and a chloride ion. [c]Reference 37. [d]Reference 21. [e]Interpolated from data of Woolf.[39]

Peptide Conformations. Cluster analyses of peptide structures present in MD trajectories of 0.1−0.3 μs duration were performed using the method described by Daura et al.[40] Peptide coordinates were taken from trajectories at intervals of 10 ps to provide coordinate sets for 10 000 to 30 000 conformations. These were clustered by comparing the rmsd's of backbone atoms. Conformations for which the rmsd from one other was less than 0.1 nm were considered to be within the same cluster. This analysis indicated that about 58% of all peptide conformations present during a simulation were represented by a single, extended β-structure, with five other similar β-structures representing about 13%, 7%, 4%, 4%, and 3% of the conformations present. Thus, by the criterion mentioned, six representative conformations of [val^5]-angiotensin account for about 90% of the conformations of the peptide present during this simulation. These backbone conformations differed mostly by small variations in conformational angles, with the largest variations present at the amino acid residues near the ends of the peptide (Figure 1). The Supporting Information provides conformational angles of these structures and fuller illustrations of them.

Three-bond spin coupling constants between peptide N−H and α-protons ($^3J_{NHC\alpha H}$) of the peptide were calculated for each snapshot of a trajectory using the Karplus-type equation provided by Vuister and Bax.[41] The averaged coupling constants obtained did not appear to depend significantly on

dx.doi.org/10.1021/jp211098v | J. Phys. Chem. B 2012, 116, 1965−1973

Figure 1. Dominant conformations of [val^5]angiotensin II in 25% methanol–water identified by a clustering study of backbone atoms. Backbone structures were superimposed for the drawing by minimizing the rmsd of backbone heavy atoms. Structures 1 through 6 (colored green, cyan, magenta, yellow, pink, and orange, respectively) had abundances of approximately 58%, 13%, 7%, 4%, 4%, and 3% during MD trajectories of 0.1–0.3 μs duration. Full drawings of these structures are given in the Supporting Information.

the length of a simulation and were close to the experimental coupling constants (Supporting Information).

Similarly, Hα proton chemical shift changes from random coil values were calculated using the dependence of shifts on the ϕ, ψ conformational angles formulated by Wishart and Nip.[42] These were averaged over the course of a trajectory. Results are given in the Supporting Information. It was found that predicted shift effects were similar for all trajectories that ranged from 0.1 to 0.3 μs duration. These conformation-dependent shift effects were in qualitative agreement with experimental results. The Wishart–Nip equations are based on experimental shift information obtained at 25 °C, and strong agreement with data produced from simulations at 0 °C probably is not expected.

Depending on peptide dynamics, intramolecular proton–proton NOEs are expected to be proportional to the average of $1/r_{i,j}^6$ or $1/r_{i,j}^3$ where $r_{i,j}$ is the internuclear distance between two protons of interest.[43] The average of $1/r_{i,j}^6$ and $1/r_{i,j}^3$ was calculated for all proton spin pairs of [val^5]angiotensin for each MD trajectory. Results of these calculations are given in the Supporting Information. It was found that the average of $1/r_{i,j}^6$ or $1/r_{i,j}^3$ was essentially independent of the duration of a MD trajectory for trajectories longer than 0.1 μs and that $1/r_{i,j}^6$ roughly correlated with observed integrated intensities of NOE cross peaks obtained in NOESY studies of the peptide. The calculations suggested that few long-range proton–proton NOEs ($>i$, $i + 1$) would likely be detectable for this system, in agreement with experimental observations.[23]

Heterogeneity of the Solvent Mixture. Examination of the faces of the simulation box (Supporting Information) emphasizes that the methanol–water solvent mixture is not homogeneous at the molecular level. In agreement with MD simulations by others that used different force fields,[44,45] and with experiment,[46,47] we find that there are clusters of water and methanol molecules throughout the simulation box. In our work, typically about 90% of the methanol molecules are associated into aggregates ranging in size from 2 to 80 molecules.

Methanol molecules within 3 nm of a peptide proton were considered when computing proton–proton spin dipolar interactions that produce intermolecular NOEs. The number of methanol molecules within this volume of interest directly influences the calculated intermolecular Overhauser effects. Figure 2A shows how the solvent composition within a sphere of 3 nm radius centered on the N–H proton of the Tyr4 residue of [val^5]angiotensin changed during a 0.3 μs simulation. Figure 2B shows composition variation around the same peptide proton on a narrower time scale. For all protons of the peptide, the number of methanol molecules relative to water molecules within the 3 nm sphere varies on time scales that

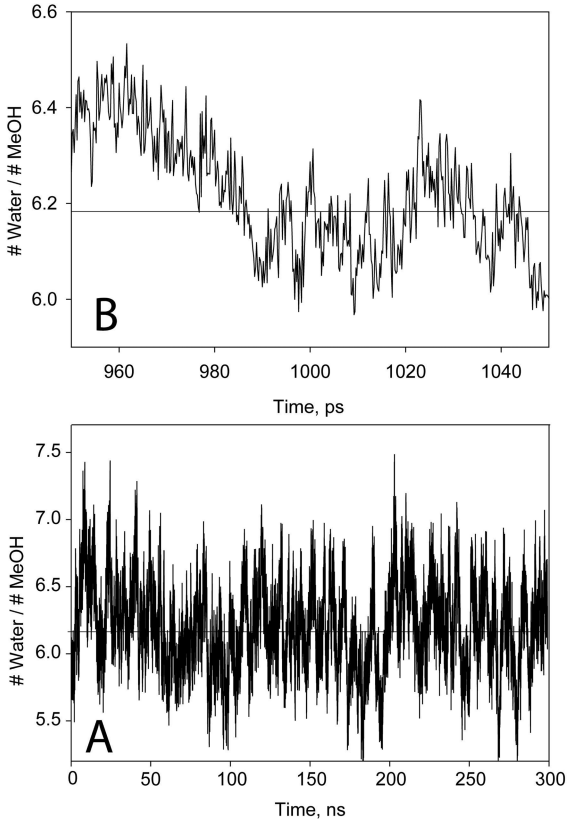

Figure 2. (A) Variation of the ratio of the number of water of molecules to methanol molecules present in a sphere of 3 nm radius centered on the Tyr4 peptide proton of [val^5]angiotensin. The configuration of the system was sampled every 10 ps. The ratio of water to methanol molecules in the bulk solution is 6.177. (B) Variation of the ratio of the number of water molecules to methanol molecules present in a sphere of 3 nm radius centered on the Tyr4 peptide proton. The configuration of the system was sampled every 0.2 ps. The data for the plots came from different simulations.

range from picoseconds to nanoseconds due to diffusion of the solvent components and the dynamics of cluster formation.

Intermolecular NOEs. The normalized correlation function $G^m(t)/G^m(0)$ for interaction of methanol CH_3 protons with a peptide proton was found to decay rapidly to a value near 0.5 in a few picoseconds, whereupon the function decayed much more slowly. The correlation function for Tyr4H-methanol interactions (Figure 3) illustrates these behaviors. Similar plots were obtained for the other protons of [val^5]angiotensin.

The quantities $G^0(0)$, $G^2(0)$, $\tau_0(\omega)$, and $\tau_2(\omega)$ which characterize the correlation functions obtained for protons of [val^5]angiotensin are collected in Table 2. The contribution of the rapid initial decay to the value of $\tau_m(\omega)$ obtained using eq 9 is small and was ignored; the values of $\tau_0(\omega)$ and $\tau_2(\omega)$ given in the table were obtained by using polyexponential fits to observed $G^m(t)/G^m(0)$ values starting at 10 ps.

Figure 4 compares cross-relaxation parameters σ_{HH}^{NOE} calculated using eq 10 and the data given in Table 2 to experimental results. The figure also shows previously reported σ_{HH}^{NOE} values obtained using eq 2 in conjunction with experimental translational diffusion coefficients and reasonable conformations of the peptide.[23] It is seen that cross-relaxation parameters predicted from simulations are about a factor of 3 larger than experimental values.

dx.doi.org/10.1021/jp211098v | J. Phys. Chem. B 2012, 116, 1965–1973

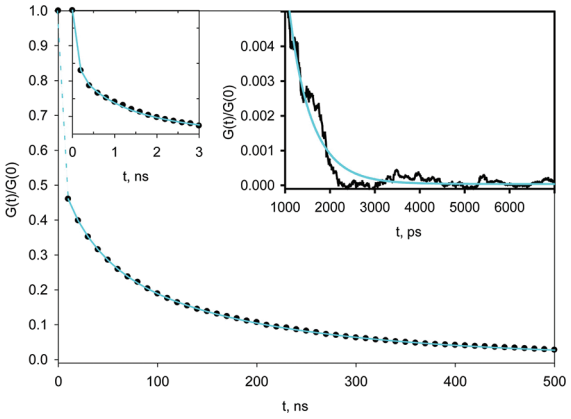

Figure 3. Behavior of the averaged computed correlation function $G^m(t)/G^m(0)$ for the Tyr4 N–H proton of [val^5]angiotensin as a function of time (black points and line). For the inset at the upper left, samples of the trajectory were taken at 0.2 ps intervals, while for the remaining curves the correlation function was sampled every 10 ps. The first few picoseconds of the function is fit by $G(t)/G(0) = 0.011 + 0.27\ \exp(-2.55t) + 0.12\ \exp(-0.066t) + 0.57\ \exp(-0.0068t)$ (cyan line). After ~20 ps, the curve is described by $4 \times 10^{-5} + 0.043\ \exp(-0.12t) + 0.22\ \exp(-0.026t) + 0.26\ \exp(-0.0060t) + 0.035\ \exp(-0.0018t)$. All time units in the equations are picoseconds.

Selective Solvent Interactions. Descriptions of intermolecular relaxation such as those of Ayant et al. (eq 2) assume that the solvent is homogeneous. In a mixed organic–water solvent, preferential accumulation of one solvent component near a peptide proton would lead to unreliable predictions of σ_{HH}^{NOE} using eq 2 since the effective value of N_S would not be the concentration characteristic of the bulk solvent.

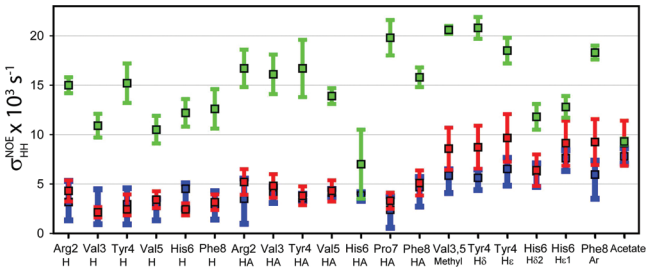

Figure 4. Experimental cross-relaxation parameters for methanol methyl proton–peptide proton interactions (red squares), average σ_{HH}^{NOE} calculated using the formulation of Ayant et al. (eq 2) (blue squares), and σ_{HH}^{NOE} computed from the MD simulations described in this paper (green squares). The red bars represent a ±25% error range for the experimental data. The blue bars correspond to the range of calculated σ_{HH}^{NOE} found for a set of ten conformations of the peptide consistent with ^{1}H–^{1}H distance constraints derived from intramolecular NOE and ROE studies. The green bars represent standard deviations of results from seven or more simulation trajectories that ranged from 0.1 to 0.3 μs in duration. The red and blue data were presented in a different format in ref 23.

Clustering of methanol and water molecules in 25% methanol–water further complicates the situation. A given proton of the peptide may find itself at some instant in a local solvent environment that is richer in methanol molecules relative to water molecules than is the case for the bulk solvent. An instant later, rearrangement of solvent molecules could present a local environment that is methanol poor. Application of eq 2 to estimating intermolecular methanol–peptide NOEs assumes that these considerations are averaged on the time scale of an NOE experiment.

Table 2. Correlation Functions and Intermolecular NOEs[a]

spin	$G^0(0) \times 10^{-3}$	$G^2(0) \times 10^{-3}$	$(G_0(0))/(G_2(0))$	fraction[b]	$\tau_0(\omega)$, ps	$\tau_2(\omega)$, ps	$\sigma_{HH}^{NOE} \times 10^2$, s^{-1}
Asp1HA	1.90 (0.15)	1.33 (0.03)	1.43	0.529 (0.010)	54.4 (2.7)	26.9 (0.6)	1.55 (0.08)
Arg2H	1.75 (0.08)	1.20 (0.05)	1.46	0.549 (0.020)	66.7 (3.4)	30.4 (0.1)	1.50 (0.08)
Arg2HA	2.09 (0.45)	1.37 (0.21)	1.52	0.547 (0.030)	64.4 (8.9)	30.0 (2.3)	1.67 (0.19)
Val3H	1.39 (0.13)	0.89 (0.08)	1.56	0.609 (0.022)	98.0 (6.0)	36.1 (0.99)	1.09 (0.12)
Val3HA	2.25 (0.26)	1.41 (0.12)	1.59	0.541 (0.027)	73.5 (10.3)	30.7 (1.09)	1.61 (0.20)
Val3CH$_3$[c]	3.03 (0.13)	2.03 (0.07)	1.49	0.492 (0.013)	48.8 (1.8)	24.0 (0.52)	2.06 (0.04)
Tyr4H	1.96 (0.24)	1.28 (0.13)	1.52	0.568 (0.020)	80.7(12.0)	32.0 (1.2)	1.52 (0.20)
Tyr4HA	2.14 (0.23)	1.46 (0.16)	1.47	0.543 (0.009)	79.5 (9.0)	30.9 (0.6)	1.67 (0.29)
Tyr4Hδ	3.06 (0.21)	2.04 (0.12)	1.50	0.506 (0.033)	53.2 (6.6)	24.7 (1.2)	2.08 (0.11)
Tyr4Hε	2.91 (0.15)	1.90 (0.11)	1.53	0.495 (0.013)	47.9 (1.5)	23.4 (0.6)	1.85 (0.13)
Val5H	1.50 (0.11)	0.98 (0.07)	1.54	0.556 (0.037)	95.4 (6.7)	33.0 (0.6)	1.05 (0.14)
Val5HA	1.83 (0.29)	1.23 (0.17)	1.49	0.543 (0.012)	87.0 (7.7)	32.1 (0.9)	1.39 (0.08)
Val5CH$_3$[c]	3.03 (0.13)	2.03 (0.07)	1.490	0.492 (0.013)	48.8 (1.8)	24.0 (0.5)	2.06 (0.04)
His6H	1.59 (0.14)	1.06 (0.10)	1.51	0.570 (0.009)	89.4 (12.9)	32.9 (2.0)	1.22 (0.14)
His6HA	0.83 (0.32)	0.56 (0.19)	1.49	0.651 (0.052)	116. (14.3)	38.9 (3.6)	0.70 (0.35)
His6Hδ2	1.68 (0.29)	1.13 (0.20)	1.48	0.537 (0.032)	57.6 (7.2)	25.9 (0.2)	1.18 (0.13)
His6Hε1	2.24 (0.18)	1.45 (0.12)	1.55	0.519 (0.034)	46.1 (7.0)	21.8 (0.9)	1.28 (0.11)
Pro7HA	2.62 (0.19)	1.85 (0.09)	1.42	0.502 (0.016)	71.6 (4.8)	28.0 (0.6)	1.98 (0.18)
Phe8H	1.37 (0.21)	0.98 (0.14)	1.41	0.574 (0.022)	80.6(1.0)	32.7 (1.5)	1.26 (0.20)
Phe8HA	1.84 (0.20)	1.27 (0.12)	1.44	0.561 (0.023)	65.7 (5.2)	30.0 (0.8)	1.58 (0.10)
Phe8Ar[d]	3.19 (0.08)	2.10 (0.07)	1.52	0.466 (0.024)	34.0 (1.6)	19.3 (0.4)	1.83 (0.07)

[a]Based on seven or more simulations of [val^5]angiotensin in 25% methanol–water (v/v) at 0 °C that produced trajectories of 0.1, 0.15, and 0.3 μs duration. Standard deviations are in parentheses. [b]The fraction of the decay of the correlation function due to slow processes. This was obtained by fitting the normalized correlation function $G^m(t)/G^m(0)$ for t over the range 10–7000 ps and then extrapolating the fitting function to $t = 0$. See Figure 3. [c]The signals for the valine methyl groups are overlapped in the experimental spectra. The values given here for these groups are averages of results for the 12 methyl protons of the peptide. [d]The values given are averages of results for the five aromatic ring protons of the Phe8.

dx.doi.org/10.1021/jp211098v | J. Phys. Chem. B 2012, 116, 1965–1973

Preferential solvent interactions with [val^5]angiotensin were explored using the MD simulation trajectories described above. We imagined four concentric spheres (Figure 5) centered on each peptide proton. The radii of the first three spheres were set at 0.4, 0.8, and 1.2 nm. (The diameter of a methanol molecule is approximately 0.4 nm.[23]) The fourth sphere had a radius of 3 nm, corresponding to the cutoff distance used in the relaxation-NOE calculations. The ratio of the number of water molecules to number of methanol molecules in each shell was calculated for each of about 100 000 snapshots taken from simulation trajectories, then averaged. Detailed results are given in the Supporting Information.

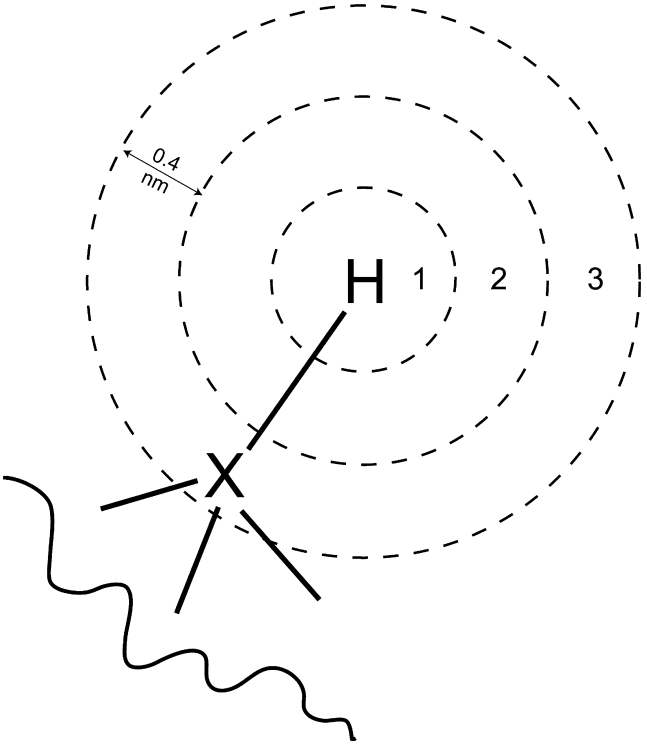

Figure 5. Selection spheres for study of possible selective solvent interactions with [val^5]angiotensin in methanol–water. A portion of each sphere is occupied by peptide.

If solvent components are homogeneously distributed, the ratio of the number of waters to number of methanols in a given volume of solvent would be 6.177. We find that this ratio ranges from 8.4 to 3.7 in solvent shell 1, the first value corresponding to a solvent shell that is preferentially water-rich over time and the latter corresponding to a solvent layer that is enriched in methanol. For each peptide hydrogen, as one moves from shell 1 to shell 3, the ratio of solvent molecules present tends to come closer to 6.177, and for solvent shell 4, which starts at a radius of 1.2 nm and extends to 3.0 nm, the composition in all cases was very close to that of bulk solvent. On average, the His6HA, His6Hε, Phe8HA, and Phe8H protons are present in a local solvent that is water-rich, while the HA protons of Asp1 and Arg2, as well as the peptide protons of Arg2 and Val3, appear to be in local environments that have essentially the same composition as the bulk solvent. The remaining protons of the peptide have local solvent environments that are, over time, enriched in methanol molecules (Supporting Information, Table 5).

Local Translational Diffusion. The derivation of eq 2 presumes that the relative motion of solute and solvent can be described in terms of the translational diffusion of these species. Their respective diffusion coefficients (D_H, D_S) are assumed to be the same throughout the sample. Due to attractive or repulsive intermolecular interactions, the rates of diffusion when species come close to each other could be different from those of molecules in the bulk solvent. Given that magnetic dipolar interactions are strongly distance-dependent, altered diffusion rates of species when they are proximate could lead to intermolecular relaxation effects different from those expected for species diffusing as in the bulk solvent.

Pettitt and co-workers have explored the mobility of water molecules near the surface of biopolymers using a difference equation (eq 11) based on the Einstein relation between mean square displacement and time.[48,49] In eq 11, $r(t)$ is the position vector of a solvent molecule at time t, and the brackets indicate averaging over time origins and all solvent molecules at a given distance from the solute proton.

$$6D = \frac{1}{(t_2 - t_1)}(\langle |r(t_2) - r(0)|^2 - |r(t_1) - r(0)|^2 \rangle) \quad (11)$$

Equation 11 was used to examine the translational mobility of methanol and water molecules that were within ~1.5 nm of the surface of [val^5]angiotensin. Simulations producing trajectories of 2 ns duration, with snapshots recorded every 0.2 ps, were used; the time ($t_2 - t_1$) was 4 ps. Some representative results are shown in Figure 6.

It was found that the translational diffusion coefficient for both solvent species was reduced about 2-fold as the solvent molecules approach backbone atoms of the peptide. At separations greater than about 1.4 nm, the diffusion coefficients were the same as those found for solvent molecules in the bulk (Table 1). Essentially the same results as shown in Figure 6 were obtained for all backbone atoms of the peptide.

Diffusion coefficients for methanol and water were also reduced as solvent molecules approached side chain protons of the peptide, but the reductions were only of the order of 25% (Figure 6). The effects on both solvent components were about the same for all side chain protons of the peptide.

DISCUSSION

The peptide–methanol–water system simulated in this work is highly heterogeneous at the microscopic level. The peptide floats in a solvent made up of clusters of water and methanol molecules. The system is also heterogeneous with regard to time, with processes taking place in the system on time scales that range from picoseconds (solvent molecule cluster formation and rearrangement) to nanoseconds (peptide conformational changes[50]) to perhaps seconds (proline *cis–trans* isomerizaton). An important question is whether or not the time period simulated is long enough that the impacts of these processes on calculated intermolecular cross-relaxation terms are appropriately averaged.

As was the case in previous work, isomerization at the proline residue was ignored in the present study.[10,23] This process is slow enough that some resolved proton NMR signals assignable to a minor (~15%) conformational isomer can be observed. However, characterizing solvent NOEs on these minor signals would be experimentally difficult at the magnetic field strength used for the experiments. There were no indications of rotation at the His6-Pro7 peptide bond in the simulations.

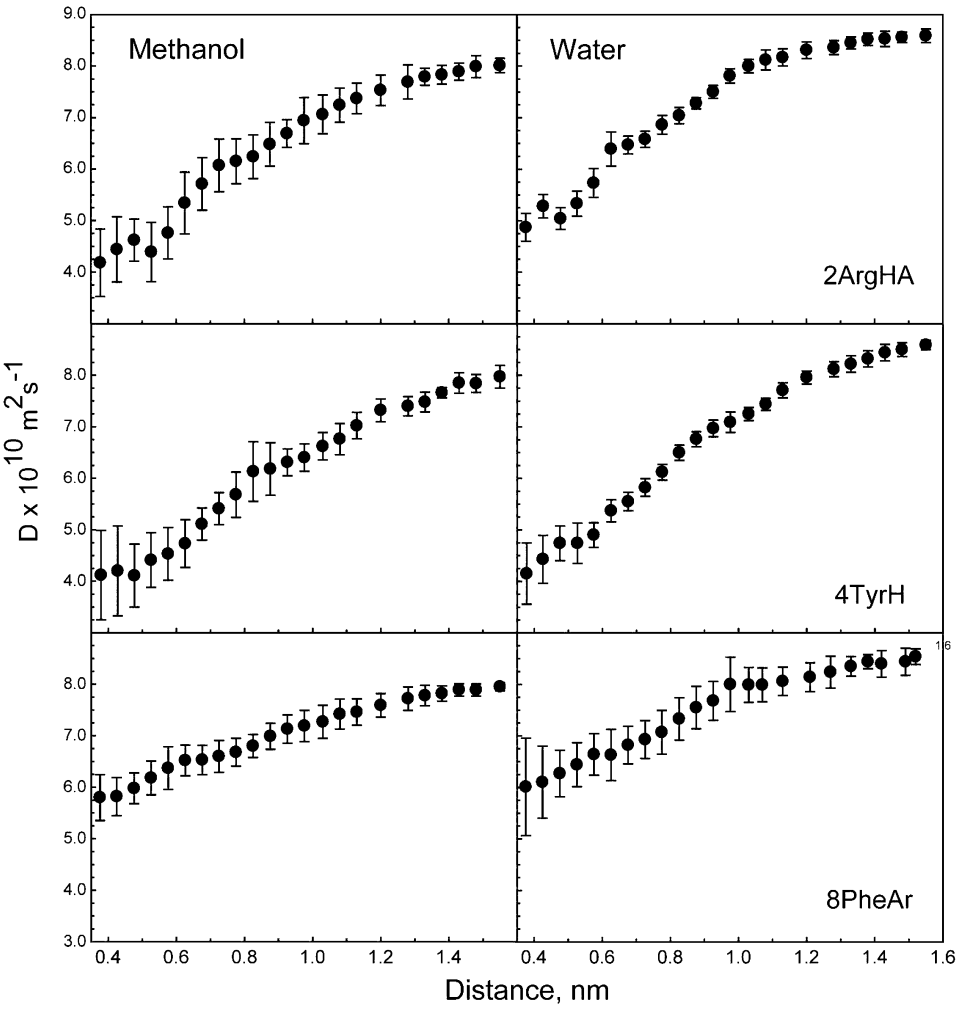

Figure 6. Dependence of the average translational diffusion coefficients of methanol (right panels) and water (left panels) as a function of distance from several protons (indicated) of [val^5]angiotensin, calculated from simulations of the peptide in 25% methanol–water (v/v) at 0 °C. The error bars indicate standard deviations.

The AMBER99SB-ILDN version of the AMBER99SB force field for peptides, in combination with the TIP4Pew water model, has been found to provide structurally and dynamically correct results in simulations that produce trajectories of up to 100 ms duration of a decapeptide[51] and of larger systems.[52,53] AMBER99SB used with other water models appears to give NMR relaxation and order parameters in good agreement with experiment.[54−56] The reliability of results obtained using the AMBER99SB parameters, in combination with those for methanol used in this work, has not been demonstrated. However, several observations suggest that conformations of [val^5]angiotensin and their interconversion are reasonably well described by the procedure used. Average values for three-bond spin coupling constants between peptide N–H and α-protons ($^3J_{\mathrm{NH}C\alpha\mathrm{H}}$) agreed fairly well with experimental values. The average did not depend on the length of the dynamics trajectory calculated as long as the length exceeded 0.1 μs. Similarly, study of distances between pairs of peptide spins gave values for the average of $1/r_{i,j}^{\,6}$ or $1/r_{i,j}^{\,3}$ that are very similar in simulations ranging from 0.1 to 0.3 μs duration. There was not quantitative agreement between the intensity of NOE cross peaks and the averaged $1/r_{i,j}^{\,6}$ or $1/r_{i,j}^{\,3}$ values, but the calculated averages were consistent with all observed intramolecular proton–proton NOEs and ROEs. Lastly, conformation-dependent chemical shift changes for the CαH protons of the peptide, calculated using parameters derived for systems at 25 °C, were qualitatively consistent with the experimental shifts observed at 0 °C. These comparisons to experimental results suggest that trajectories longer than 0.1 μs produced by simulations of [val5]angiotensin in 25% methanol–water at 0 °C sufficiently sample and average the conformational changes of the peptide and the reorganizations of its solvent environment, so that reliable estimates of intermolecular relaxation effects can be expected.

Preto et al. have reported simulations of angiotensin II at 27 °C in explicit TIP3P water or OPLS dimethylsulfoxide solvents.[21] An AMBER force field (presumably AMBER94) was used for the peptide. The distributions of phi–psi backbone conformational angles for the Arg2 residue found in our work (given in the Supporting Information) are qualitatively similar to the same data provided by Preto et al. As expected, the number of dihedral angle transitions per unit time observed in our work at 0 °C is lower than is apparent at 27 °C in the results of Preto et al. (Also, rates of dihedral transitions produced using AMBER94 appear to be larger than those obtained using AMBER99SB.[55]) These authors found the peptide N-terminus to be more mobile than the C-terminus in water but not in DMSO. Our simulations indicate that in

dx.doi.org/10.1021/jp211098v | J. Phys. Chem. B 2012, 116, 1965–1973

methanol–water interior residues of the peptide have lower rates of backbone dihedral angle transitions than do residues at the peptide termini but that there is not a large difference in the mobility of N- and C-terminal residues.

The peptide–solvent model used in our work leads to predicted translational diffusion coefficients that are too large by about 50% (Table 1). Overestimation of diffusion coefficients by MD simulations is common. Using the OPLS model for methanol and TIP4P water, simulations by Wensink et al. produced diffusion coefficients for methanol and water in mixtures that were ~80% too large.[57] Similarly, with a propriety force field, Chowdhuri and Chandra found that diffusion coefficients of methanol and water predicted from simulations of mixtures were too large over the entire range of composition.[58] An early GROMOS force field for methanol in combination with the SPC/E model for water[59] and work done with the GROMOS96 force field and the SPC water model[60] overestimated diffusion coefficients for components of methanol–water mixtures. The number of molecules used in these simulations varied; it has been found that diffusion coefficients obtained from simulations can depend on the number of molecules present in the simulation, with calculations involving larger numbers of molecules tending to produce greater disagreement with experimental values.[13,59]

The very rapidly decaying initial component of the correlation functions for methanol–peptide interactions (Figure 4) is characterized by lifetime (τ_m) ranging from 0.5 to 15 ps. Rotational diffusion of methyl groups has been described using a rotational diffusion constant (D_r) of about 2×10^{10} s^{-1} at 273 °C,[61] corresponding to a lifetime τ ($\approx 1/6D_r$) of 8 ps.[62] It is reasonable to assign the processes producing the rapid decay of the correlation functions to rotation and libration of methanol molecules.

Values of $G^0(0)$ and $G^2(0)$ found for correlation functions for peptide proton–methanol proton interactions depend on the number of methanol methyl hydrogens within the 3 nm radius selection sphere used *and* the arrangement of those hydrogens within that sphere. Methanols within the sphere that can closely approach peptide protons will make a larger contribution to $G^0(0)$ and $G^2(0)$ per methanol hydrogen than methanol molecules that are more distant. Consistent with this expectation, hydrogens on the side chains of the residues 3 to 8 (excepting Pro7) exhibit $G^0(0)$ and $G^2(0)$ values larger than those of the corresponding backbone hydrogens. Calculations using the NACCESS program[63] showed that side chain protons of [val^5]angiotensin structures represented in Figure 1 typically have 2–3 times more solvent-exposed surface area than backbone protons.

It is unfortunate that an experimental value for the intermolecular NOE on the His6HA proton cannot be obtained due to the near-coincidence of the chemical shift of this proton and the water resonance. The computed $G^0(0)$ and $G^2(0)$ values for this proton are strikingly smaller than those for other peptide backbone or side chain protons (Table 2). Solvent-exposed surface areas for the His6HA proton are zero or near-zero in all of the conformations shown in Figure 1. The implications of the surface area calculation are buttressed by the calculations of selective solvation described earlier. Those showed that methanol is preferentially excluded from the environment immediately around this proton. The rapid initial decay of the His6HA correlation function is less for this proton than for others of the peptide (Table 2). If the initial decay is indeed due to motions of nearby methanol molecules, this observation is consistent with a reduced presence of methanol in the vicinity of the His6HA proton. Examination of conformations represented in Figure 1 suggests that solvent approaches to His6HA are inhibited by side chains of Tyr4 and Pro7.

Near-neighbor solvent interactions with Phe8H, Phe8HA, and 6HISHε1 also preferentially exclude methanol molecules. Values of $G^0(0)$ and $G^2(0)$ seem to be somewhat less for these protons compared to others in the peptide but not dramatically so.

There is poor agreement between experimental cross-relaxation terms (σ_{HH}^{NOE}) and those predicted from MD simulations (Figure 5). However, the simulations predict that (1) σ_{HH}^{NOE} for all protons of [val^5]angiotensin are of the same order of magnitude, (2) σ_{HH}^{NOE} for peptide backbone protons are similar to each other, and (3) the cross-relaxation parameters for protons of the amino acid side chains are somewhat larger than those for the backbone protons. Except for the His6 ring protons, these trends are consistent with experimental observations. Given the dependence of σ_{HH}^{NOE} on translational diffusion of the system components (eqs 1 and 2), it seems unlikely that better agreement of observed and calculated cross-relaxation terms will be achieved until simulations can more accurately predict translational diffusion coefficients. Including polarization effects in MD force fields has been found to improve the reliability of diffusion coefficients, albeit at a considerable increase in needed computational resources.[64−67] It has been shown that inclusion of polarization effects using a fluctuating charge formalism leads to translational diffusion coefficients of both methanol and water in methanol–water mixtures at 25 °C that are smaller than the experimental values.[68] Inclusion of polarization could be effective in producing better estimates of translational diffusion coefficients and cross-relaxation terms for the system examined here.

■ ASSOCIATED CONTENT

Supporting Information

Illustrations of the simulation box used and the structures represented in Figure 1, computed vicinal coupling constants, HA chemical shift increments and intraresidue H–H distances, solvent abundances in the solvent shells indicated in Figure 5, and details of conformational angle changes at Arg2. This material is available free of charge via the Internet at http://pubs.acs.org.

■ AUTHOR INFORMATION

Corresponding Author

*Phone: 805-893-2113. Fax: 805-893-4120. E-mail: gerig@nmr.ucsb.edu.

Notes

The authors declare no competing financial interest.

■ ACKNOWLEDGMENTS

We thank the National Science Foundation for support of the initial phases of this work (Grant CHE-0408415) and the authors and developers of GROMACS for making their software available.

■ REFERENCES

(1) Hudson, E. P.; Eppler, R. K.; Beaudoin, J. M.; Dordick, J. S.; Reimer, J. A.; Clark, D. S. *J. Am. Chem. Soc.* **2009**, *131*, 4294.

(2) Tournier, A. L.; Reat, V.; Dunn, R.; Daniel, R.; Smith, J. C.; Finney, J. *Phys. Chem. Chem. Phys.* **2005**, *7*, 1388.
(3) Chaudhary, N.; Singh, S.; Nagaraj, R. *J. Pept. Sci.* **2009**, *15*, 675.
(4) Gerig, J. T.; Strickler, M. A. *Biopolymers* **2002**, *64*, 227.
(5) Angulo, M.; Hawat, C.; Hofmann, H.-J.; Berger, S. *Org. Biomol. Chem.* **2003**, *1*, 1049.
(6) Neuman, R. C. Jr.; Gerig, J. T. *Magn. Reson. Chem.* **2009**, *47*, 925.
(7) Gerig, J. T. *Biophys. J.* **2004**, *86*, 3166.
(8) Gerig, J. T. *Biopolymers* **2004**, *74*, 240.
(9) Gerig, J. T. *J. Phys. Chem. B* **2008**, *112*, 7967.
(10) Neuman, R. C. Jr.; Gerig, J. T. *J. Phys. Chem. B* **2011**, *115*, 1712.
(11) Ayant, Y.; Belorizky, E.; Fries, P.; Rosset, J. *J. Phys. (Paris)* **1977**, *38*, 325.
(12) Luhmer, M.; Moschos, A.; Reisse, J. *J. Magn. Reson. A* **1995**, *113*, 164.
(13) Gerig, J. T. *J. Magn. Reson.* **2011**, *210*, 171.
(14) Kobori, H.; Nangaku, M.; Navar, L. G.; Nishiyama, A. *Pharmacol. Rev.* **2007**, *59*, 251.
(15) Timmermans, P. B.; Wong, P. C.; Chiu, A. T.; Herblin, W. F.; Benfield, P.; Carini, D. J.; Lee, R. J.; Wexler, R. R.; Saye, J. A.; Smith, R. D. *Pharmacol. Rev.* **1993**, *45*, 205.
(16) Paul, M.; Mehr, A. P.; Kreutz, R. *Physiol. Rev.* **2006**, *86*, 747.
(17) Collet, O.; Premilat, S. *Int. J. Pept. Protein Res.* **1996**, *47*, 239.
(18) Garcia, K. C.; Ronco, P. M.; Verroust, P. J.; Brunger, A. T.; Amzel, L. M. *Science* **1992**, *257*, 502.
(19) D'Amelio, N.; Gaggelli, E.; Gaggelli, N.; Lozzi, L.; Neri, P.; Valensin, D.; Valensin, G. *Biopolymers* **2003**, *70*, 134.
(20) Tzakos, A. G.; Bonvin, A. M. J. J.; Troganis, A.; Cordopatis, P.; Amzel, M. L.; Gerothanassis, I. P.; van Nuland, N. A. *Eur. J. Biochem.* **2003**, *270*, 849.
(21) Preto, M. A. C.; Melo, A.; Maia, H. L. S.; Mavromoustakos, T.; Ramos, M. J. *J. Phys. Chem. B* **2005**, *109*, 17743.
(22) Chatterjee, A.; Bothra, A. K. *Int. J. Integr. Biol.* **2010**, *9*, 21.
(23) Neuman, R. C. Jr.; Gerig, J. T. *J. Phys. Chem. B* **2010**, *114*, 6722.
(24) van der Spoel, D.; Lindahl, E.; Hess, B.; Groenhof, G.; Mark, A. E.; Berendsen, H. J. C. *J. Comput. Chem.* **2005**, *26*, 1701.
(25) Hess, B.; Kutzner, C.; van der Spoel, D.; Lindahl, E. *J. Chem. Theory Comput.* **2008**, *4*, 435.
(26) Hornak, V.; Abel, R.; Okur, A.; Strockbine, B.; Roitberg, A.; Simmerling, C. *Proteins: Struct., Func., Genet.* **2006**, 65.
(27) Lindorff-Larsen, K.; Piana, S.; Palmo, K.; Maragakis, P.; Klepeis, J. L.; Dror, R. O.; Shaw, D. E. *Proteins* **2010**, *78*, 1950.
(28) Thurlkill, R. L.; Grimsley, G. R.; Scholtz, J. M. *Protein Sci.* **2006**, *15*, 1214.
(29) Cornell, W. D.; Cieplak, P.; Bayly, C. I.; Kollman, P. A. *J. Am. Chem. Soc.* **1993**, *115*, 9620.
(30) Horn, H. W.; Swope, W. C.; Pitera, J. W.; Madura, J. D.; Dick, T. J.; Hura, G. L.; Head- Gordon, T. *J. Chem. Phys.* **2004**, *120*, 9665.
(31) Allen, M. P.; Tildesley, D. J. *Computer simulations of liquids*; Oxford: Oxford, 1987.
(32) Grabuleda, X.; Jaime, C.; Kollman, P. A. *J. Comput. Chem.* **2000**, *21*, 901.
(33) Leach, A. R. *Molecular Modeling-Principles and Applications*, 2nd ed.; Pearson Prentice Hall: Harlow, England, 2001.
(34) Abragam, A. *The principles of nuclear magnetism*; Oxford: Oxford, 1961.
(35) Lippens, G.; Van Belle, D.; Wodak, S. J.; Jeener, J. *Mol. Phys.* **1993**, *80*, 1469.
(36) Odelius, M.; Laaksonen, A.; Levitt, M. H.; Kowalewski, J. *J. Magn. Reson. A* **1993**, *105*, 289.
(37) Feller, S. E.; Huster, D.; Gawrisch, K. *J. Am. Chem. Soc.* **1999**, *121*, 8963.
(38) Provencher, S. W. *J. Chem. Phys.* **1976**, *64*, 2772.
(39) Woolf, L. A. *Pure Appl. Chem.* **1985**, *57*, 1083.
(40) Daura, X.; Gademan, K.; Juan, B.; Seebach, D.; van Gunsteren, W. F.; Mark, A. E. *Angew. Chem., Int. Ed.* **1999**, *38*, 236.
(41) Vuister, G. W.; Bax, A. *J. Am. Chem. Soc.* **1993**, *115*, 7772.
(42) Wishart, D. S.; Nip, A. M. *Biochem. Cell. Biol.* **1998**, *76*, 153.
(43) Neuhaus, D.; Williamson, M. P. *The Nuclear Overhauser Effect in Structural and Conformational Analysis*, 2nd. ed.; Wiley-VCH: New York, 2000.
(44) Dougan, L.; Hargreaves, R.; Bates, S. P.; Finney, J. L.; Reat, V.; Soper, A. K.; Crain, J. *J. Chem. Phys.* **2005**, *122*, 174514.
(45) Allison, S. K.; Fox, J. P.; Hargreaves, R.; Bates, S. P. *Phys. Rev. B* **2005**, *71*, 024201.
(46) Dixit, S.; Crain, J.; Poon, W. C. K.; Soper, A. K. *Nature* **2002**, *416*, 829.
(47) Dixit, S.; Soper, A. K.; Finney, J. L.; Crain, J. *Europhys. Lett.* **2002**, *59*, 377.
(48) Lounnas, V.; Pettitt, B. M.; Phillips, G. N. Jr. *Biophys. J.* **1994**, *66*, 601.
(49) Makarov, V. A.; Feig, M.; Andrews, B. K.; Pettitt, B. M. *Biophys. J.* **1975**, *75*, 150.
(50) Gnanakaran, S.; Nymeyer, H.; Portman, J.; Sanbonmatsu, K. Y.; Garcia, A. E. *Curr. Opin. Struct. Biol.* **2003**, *13*, 168.
(51) Fawzi, N. L.; Phillips, A. H.; Ruscio, J. Z.; Doucleff, M.; Wemmer, D. E.; Head-Gordon, T. *J. Am. Chem. Soc.* **2008**, *130*, 6145.
(52) Shaw, D. E.; Maragakis, P.; Lindorff-Larsen, K.; Piana, S.; Dror, R. O.; Eastwood, M. P.; Bank, J. A.; Jumper, J. M.; Salmon, J. K.; Shan, Y.; Wriggers, W. *Science* **2010**, *330*, 341.
(53) Piana, S.; Sarkar, K.; Lindorff-Larsen, K.; Guo, M.; Gruebele, M.; Shaw, D. E. *J. Mol. Biol.* **2011**, *405*, 43.
(54) Showalter, S. A.; Brushweiler, R. *J. Chem. Theory Comput.* **2007**, *3*, 961.
(55) Aliev, A. E.; Courtier-Murias, D. *J. Phys. Chem. B* **2010**, *114*, 12358.
(56) Calligari, P.; Calandrini, V.; Kneller, G. R.; Abergel, D. *J. Phys. Chem. B* **2011**, *115*, 12370.
(57) Wensink, E. J. W.; Hoffmann, A. C.; van Maaren, P. J.; van der Spoel, D. *J. Chem. Phys.* **2003**, *119*, 7308.
(58) Chowdhuri, S.; Chandra, A. *J. Chem. Phys.* **2005**, *123*, 234501.
(59) van de Ven-Lucassen, I. M. J. J.; Vlugt, T. J. H.; van der Zanden, A. J. J.; Kerkhof, P. J. A. M. *Mol. Simul.* **1999**, *23*, 79.
(60) Farhadian, N.; Shariaty-Niassar, M. *Iran. J. Chem. Eng.* **2009**, *6*, 62.
(61) Ericsson, A.; Kowalewski, J.; Stilbs, P. *J. Magn. Reson.* **1980**, *38*, 9.
(62) Noggle, J. H.; Schirmer, R. E. *The Nuclear Overhauser Effect*; Academic: New York, 1971.
(63) Hubbard, S. J.; Thornton, J. M. *NACCESS, Dept. of Biochemistry and Molecular Biology*, Univ. College: London, 1993.
(64) Yan, T.; Burnham, C. J.; Del Popolo, M. G.; Voth, G. A. *J. Phys. Chem. B* **2004**, *108*, 11877.
(65) Rey-Castro, C.; Vega, L. F. *J. Phys. Chem. B* **2006**, *110*, 14426.
(66) Geerke, D. P.; Van Gunsteren, W. F. *Mol. Phys.* **2007**, *105*, 1861.
(67) Borodin, O. *J. Phys. Chem. B* **2009**, *113*, 11463.
(68) Zhong, Y.; Warren, G. L.; Patel, S. *J. Comput. Chem.* **2008**, *29*, 1142.